Biochimica et Biophysica Acta, 599 (1980) 639—651

BBA 78728

TEMPERATURE-DEPENDENT RELATIONSHIP BETWEEN K^+ INFLUX, Mg^{2+}-ATPase ACTIVITY, TRANSMEMBRANE POTENTIAL AND MEMBRANE LIPID COMPOSITION IN MYCOPLASMA

C. LE GRIMELLEC and G. LEBLANC

Department of Medicine, University of Montreal and Research Center, Maisonneuve-Rosemont Hospital, 5415 L'Assomption Boulevard, Montreal PQ H1T 2M4 (Canada) and Department of Biology, C.E.N. Saclay, Gif-sur-Yvette 91190, BP 2 (France)

(Received July 6th, 1979)
(Revised manuscript received December 17th, 1979)

Key words: K^+ transport; ATPase; Membrane lipid; Transmembrane potential; (Mycoplasma)

Summary

The temperature-dependent relationship between K^+ active influx, Mg^{2+}-ATPase activity, transmembrane potential ($\Delta\Psi$) and the membrane lipid composition has been investigated in mycoplasma PG3. Native organisms were grown in a medium containing 10 μg/ml cholesterol and either oleic plus palmitic (chol (+), O + P) or elaidic (chol (+), E) acids. Adapted cells were grown in a medium free of exogenous cholesterol and supplemented with elaidic acid (chol (—), E).

Arrhenius plots of $^{42}K^+$ active influx gave a linear relationship for (chol (+), O + P) cells ($E_A = -9$ kcal). On the other hand, when oleic plus palmitic acids are replaced by elaidic acid, an upward discontinuity appears between 28 and 30°C, which is associated with a large increase in the apparent activation energy of the process ($t > 30$°C, $E_A = -24$ kcal; $t < 30$°C, $E_A = -40$ kcal).

Finally, a biphasic response with a break at approx. 23°C ($E_A = -7$ kcal, $t > 23$°C; $E_A = -44$ kcal, $t < 23$°C) is observed for (chol (—), E) organisms. From the lack of correspondence between these effects on the K^+ influx and the temperature dependence of both the Mg^{2+}-ATPase activity and $\Delta\Psi$, it is suggested that changes in the membrane lipid composition affect the K^+ transport at the level of the K^+ carrier itself.

Differential scanning calorimetry, steady-state fluorescence polarization of diphenylhexatriene and freeze-fracture electron microscopy experiments further suggest that the effect is largely due to modifications of the membrane

Abbreviation: SDS, sodium dodecyl sulfate.

microviscosity and that the K^+ carrier is associated with the most fluid lipid species present in the membrane.

Introduction

Experimental data accumulated from the last 10 years indicate that changes in the plasma membrane lipid composition affect the activity of various membrane enzymes and transport systems [1—4]. Although a large part of the available information comes from prokaryotic organisms, the relationship between their membrane lipid composition and physical state and their ionic transport systems remains obscure. The present study was undertaken to investigate such a possible lipid dependence of the K^+ active transport system in *Mycoplasma mycoides* sp. *capri* (PG3).

Mycoplasma PG3 accumulates K^+ against a large concentration gradient [5]. The steady-state intracellular K^+ level is accounted for by the value of a transmembrane potential ($\Delta\Psi$) created by the activity of a membrane-bound Mg^{2+}-ATPase [6]. Membrane cholesterol concentrations and fatty acid composition can be drastically altered in PG3 [7]. Using this particular property, it has been shown that at 37°C, the intracellular K^+ level of PG3 could be modulated by the cholesterol content of the membrane [8]. This process, however, appears to be indirect and mediated by a modification in $\Delta\Psi$. In the present work, the temperature-dependent relationship between K^+ active influx, Mg^{2+}-ATPase activity, $\Delta\Psi$ and the membrane physical state has been studied. Our results strongly suggest that the K^+ carrier is associated with the molecular lipid species with the lowest transition temperature and is sensitive to the changes in the membrane physical state.

Materials and Methods

Organisms and growth conditions. Native and low cholesterol adapted organisms were grown on modified Edward's medium [9] in which 0.5% fatty acid-deficient bovine serum albumin (Miles Laboratories Inc., Kankakee, IL) was used to replace the PPLO serum fraction. For native organisms, the medium was supplemented with 10 μg/ml cholesterol and sodium salts of either oleic plus palmitic acids (5 μg/ml each) or elaidic acid (10 μg/ml). The medium used for adapted organisms contained 10 μg/ml elaidic acid but cholesterol was omitted.

Organisms were grown statically for 14—18 h and in each case collected by centrifugation (8000 × *g*, 10 min) during the early log phase. They were washed once with cold 0.25 M NaCl solution containing 0.01 M $MgCl_2$. $MgCl_2$ was omitted from the washing solution when membranes had to be prepared.

Intracellular K^+ content and unidirectional fluxes. Intracellular K^+ of washed organisms collected from the growth or the transport assay medium was determined by flame photometry after solubilization of cells by sodium dodecyl sulfate. Initial rates of active K^+ exchange influx were measured under steady-state conditions in a buffer containing: 0.1 M phosphate; 35 mM NaCl; 2 mM $MgCl_2$; 1 mM KCl; 20 mM glucose, pH 7.2. After a 5 min preincubation period

at the chosen temperature, the assay was started by adding 2.5 μCi $^{42}K^+$ (CIS, CEA, France) per ml of cell suspension (approx. 1 mg cell protein/ml). At various times, from 45 s to 15 min, 0.1 ml samples of this cell suspension were collected, diluted in 1 ml ice-cold NaCl/Mg^{2+} solution, filtered through HA 45 Millipore filters under a negative pressure of 60—70 mmHg and washed with 5-ml of the ice-cold solution. 5-ml H_2O were added to the filters once they were transferred into glass scintillation vials for counting using Cerenkov radiation. Effectiveness of the steady-state conditions was checked by comparing the intracellular K^+ values before and after the unidirectional flux experiments.

Membrane preparation. Membranes were prepared by osmotic lysis according to the method of Rottem et al. [10], resuspended in diluted (1 : 20) β-buffer 0.15 M NaCl, 0.05 M Tris, 0.01 M 2-mercaptoethanol, pH 7.4) and kept at —45°C until used (generally within 2 or 3 days).

Enzyme assay. ATPase activity was measured by the release of P_i from the reaction mixture which contained 5 mM $MgCl_2$, 50 mM Tris-HCl (pH 8.0), 4.4 mM NaCl and 50—150 μg membrane protein/ml. The reaction was started by adding 1.25 μM radioactively labelled ATP ([γ-^{32}P]ATP, 0.5 μCi/ml; Amersham) [8,11]. Samples of 0.15 ml were collected at various times (from 2 to 15 min) and the reaction stopped with 0.3 ml of a solution containing 25% activated charcoal in 5% trichloroacetic acid. After centrifugation (10 000 $\times$ g, 2 min), part of the supernatant was collected, directly transferred into vials containing Instagel (Packard R) and counted. Liberated P_i was calculated from the known specific activity. ATPase activity was calculated from the linear part of the curves.

Fluorescence measurements. Fluorescence measurements were performed on 2-ml samples contained in a quartz fluorescence cuvette. The cuvette was held in the thermostatically maintained cell compartment, connected to a Nesslab temperature programmable circulatory bath of an Aminco Bowman spectrofluorimeter. Temperature was monitored with a thermolinear probe (YSI 729) immersed in the solution which was stirred with a magnetic stirrer. In some experiments, a Perkin Elmer MPF 44A spectrofluorimeter was used.

Variations in the transmembrane potential were calculated from changes in the merocyanine fluorescence intensity as previously described [6]. Briefly, $5 \cdot 10^{-6}$ M merocyanine 540 (Eastman Kodak Co., Rochester, NY) was added to resting organisms resuspended in the phosphate buffer (approx. 250 μg protein/ml). After a 5 to 10 min equilibration period at 37°C, the fluorescence intensity level of resting cells was recorded (λ_{exc} = 540 nm, λ_{em} = 582 nm). Addition of glucose (20 mM) induces a rapid (1—2 min) and large (20—30%) drop in the fluorescence intensity of resting cells [6]. Once the plateau was obtained, temperature was continuously decreased to 12—15°C (1—2°C/min) and the fluorescence intensity simultaneously recorded. Reversibility was checked by returning the temperature to 37°C. Temperature-dependent determinations of the fluorescence intensity of non-energized cells were performed either simultaneously (Perkin Elmer) or successively (Aminco Bowman). Results from both methods were identical and are expressed as the percentage of quenching $(\Delta F/F)\theta$ at a given temperature, θ, over the fluorescence intensity quenching measured at 37°C $(\Delta F/F)_{37°C}$ where ΔF = fluorescence intensity of resting cells minus fluorescence intensity in the energized state and F = the

fluorescence intensity of resting cells for a determined temperature.

For steady-state fluorescence polarization measurements, the excitation beam was polarized by a Thompson glan prism. The emission pathway was equipped with polarizing film (HN 38, Polaroid Co., Cambridge, MA) mounted as described by Chen and Bowman [12]. 1,6-Diphenyl-1,3,5-hexatriene (Aldrich) was excited at 365 nm (bandwidth 11 nm) and emission observed at 450 nm after passing through a 3-73 Corning or a 2 A Kodak cut-off filter. Corrections for the contribution of the scattered light were performed according to the method of Shinitzky et al. [13]. Fluorescence labelling of membranes was achieved by preincubating a membrane suspension (100—200 μg membrane protein/ml in phosphate buffer) in the presence of 2—4 μM diphenylhexatriene for 90 min at 37°C.

Differential scanning calorimetry. Differential scanning calorimetry (DSC) experiments were performed on a Perkin Elmer DSC-2B apparatus operating at a scan rate of 5 or 10°C/min. Samples (0.5—1.0 mg membrane protein) from a thick membrane suspension obtained by centrifugation (100 000 × g, 90 min) were transferred into 20-μl aluminum pans (Perkin Elmer), sealed, and scanned at least three times from 0 to 60°C. The reference pan was filled with either diluted β-buffer or Al_2O_3.

Freeze-fracture electron microscopy. Freeze-fracture experiments were performed on organisms fixed at 37, 27 and 7°C in a glutaraldehyde-isosmotic phosphate solution (final glutaraldehyde concentration 1%), as previously described [8].

Analytical methods. Lipids were extracted from whole cells or membrane suspensions according to the method of Bligh and Dyer [14] and treated as previously described [8]. Methyl esters of fatty acids [15] were subjected to gas-liquid chromatography in a Packard apparatus (Model 802, column: 10% Silar on 100/120 gas-chrom Q, Applied Science Lab. Inc., State College, PA, 180°C, N_2 = 35 ml/min). Fatty acids were identified by their retention times. Cholesterol was determined chemically by following the method of Wycoff and Parsons [16]. Proteins were determined according to the method of Lowry et al. [17] using bovine serum albumin as standard.

Results

As expected from previous reports [7,8], the membrane fatty acid composition of PG3 organisms is dependent on the fatty acid species added to the growth medium (Table I). Adaptation of native cells in a medium free of exogenous cholesterol reduces by more than 10-fold the cholesterol content of the membrane.

K^+ transport. Arrhenius plots of K^+ active influx in normal- and low-cholesterol organisms are presented in Fig. 1. Three different patterns can be observed corresponding to the three different lipid compositions studied: for (chol (+), O + P) organisms, the apparent activation energy (E_A) is low (—9.0 kcal) and constant over the range of temperatures studied. Replacement of oleic plus palmitic acids by elaidic acid results in a large increase in E_A associated with the appearance of an upward deflection at approx. 30°C. According to the cell batch, the width of the discontinuity varied from 2 to 5°C. E_A

TABLE I

MEMBRANE CHOLESTEROL AND FATTY ACID COMPOSITION OF POLAR LIPIDS

Organisms were grown in modified Edward's medium containing 10 μg/ml cholesterol (chol (+)) or no added cholesterol (chol (—)). Fatty acids were given as sodium salts.

	Cholesterol (μg/mg membrane protein)	Fatty acids (mol%)							
		12:0	14:0	16:0	16:1	18:0	$18:1_c$	$18:1_t$	18:2
Chol (+), O + P	95	0.5	0.5	57.3	0.2	4.3	35.7	—	1.5
Chol (+), E	80	0.6	0.7	8.9	2.4	14.7	—	66.6	5.7
Chol (—), E	8.3	0.1	2.0	12.3	0.7	9.0	—	72.9	2.4

values ranged from —24 to —33 kcal for temperatures above 30°C and from —30 to —45 kcal/mol on the lower end of the discontinuity, i.e., three to five times that of oleic plus palmitic cells. In spite of comparable intracellular K^+ values at 37°C (42 μg/mg protein for oleic plus palmitic acid and 40 μg/mg protein for elaidic acid), the rate of active K^+ influx is significantly depressed in these elaidate organisms. Suppression of cholesterol in the growth medium restores a high rate of K^+ active influx for temperatures higher than 25°C with an apparent activation energy comparable to that of (chol (+), O + P) cells (—7 kcal/mol). This allows the exclusion of a specificity of either the fatty acid composition or the cholesterol content in the observed temperature dependence of K^+ active influx. Below this temperature of 25°C, which corresponds to the lower end of a lipid phase transition (see below), a large increase in the activation energy occurs (—44 kcal/mol) which further demonstrates the sensi-

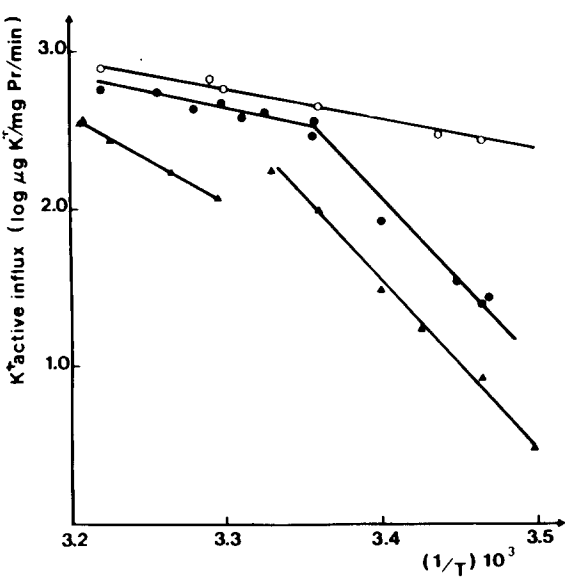

Fig. 1. Arrhenius plots of $^{42}K^+$ active influx as function of membrane lipid composition. ○, (chol (+), O + P); ▲, (chol (+), E); ●, (chol (—), E). Cells were collected during the early log phase and assayed for $^{42}K^+$ active influx as described in Methods.

tivity of the K^+ active influx towards the lipid physical state.

Mg^{2+}-ATPase activity. The Mg^{2+}-ATPase of mycoplasma PG3 is a membrane-bound enzyme the activity of which is influenced by the physical state of the membrane lipids [18]. In the present experiments, a change in the slope of the ATPase activity vs. temperature plot was observed at approx. 30°C for the three membrane compositions studied (Fig. 2). Activation energy for (chol (+), O + P) was −5 ± −0.5, for (chol (+), E) −13 ± 1.5 and for (chol (−), E) −4.7 ± 1 kcal/mol at $t > 30$°C; and −25.5 ± 2.2, 26 ± 1.7 and 28.4 ± 3.5, respectively, at $t < 30$°C. It should be noted that nowhere was an upward deflection in the Arrhenius plot of the ATPase activity of (chol (+), E) cells observed, and that in low-cholesterol cells, the temperature of the break in the ATPase and K^+ transport curves did not correspond.

Transmembrane potential. Variations in the fluorescence intensity of merocyanine 540 can be used in PG3 native organisms to monitor the relative changes in $\Delta\Psi$ [6]. Although cholesterol-depleted cells at 37°C show a $\Delta\Psi$ value only slightly reduced compared to that of normal cholesterol cells [8], attempts to monitor this $\Delta\Psi$ by using merocyanine 540 failed. This is most likely to be related to the changes in the membrane composition. Thus, it has been observed that using the same concentration of dye on (chol (+)) non-energized cells, the basal fluorescence level obtained with oleic plus palmitic acids was approx. 2-fold that of elaidate (51.2 vs. 27.5, arbitrary units). Similarly, attempts to monitor $\Delta\Psi$ by using merocyanine 540 on *Acholeplasma laidlawii* organisms or membrane vesicle preparations from *Escherichia coli* also proved unsuccessful (Le Grimellec and Leblanc, unpublished data).

In spite of the aforementioned differences in the basal level, the addition of glucose to (chol (+)) organisms at 37°C results in a comparable drop of the fluorescence intensity in oleic plus palmitic acids ($\Delta F/F$ = 26%) and elaidic acid ($\Delta F/F$ = 27%), in accordance with the observation that at 37°C, $\Delta\Psi$ as determined by the use of valinomycin is similar for both membrane compositions (−130 to −145 mV, negative inside) [8]. Temperature dependence of the fluorescence quenching induced by energization of the cells is presented in

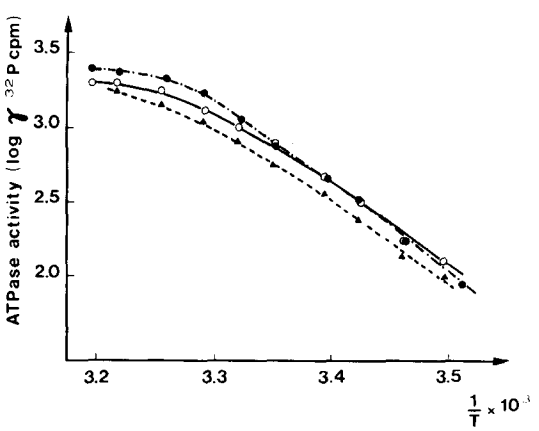

Fig. 2. Arrhenius plots of membrane ATPase activity in native and adapted PG3 organisms. Symbols as in Fig. 1.

Fig. 3. Lowering the temperature from 37 to 30°C only reduces the relative quenching by 3 and 5% for elaidic and oleic plus palmitic cells, respectively. Below the 28—30°C range, the effect of temperature becomes more pronounced but remains limited. Values obtained at 15°C represent 75% (elaidic) and 63% (oleic plus palmitic) of controls. No net upward deflection within the 30—25°C range was observed for (chol (+), E) cells.

Differential scanning calorimetry. Thermograms of membranes prepared from organisms grown in the three different media are presented in Fig. 4. A large and broad reversible endothermic transition between 20 and 48°C is observed for low-cholesterol elaidate membranes. The presence of 10% stearic acid in the membrane probably accounts for the shift in the transition temperature range which is 5 to 8°C higher than that reported for *A. laidlawii* enriched with 18 : 1 *t* [19]. On the other hand, no clear phase transition could be detected within the 10—50°C range for native cells grown with either elaidic or oleic plus palmitic acids.

Fluorescence polarisation. Steady-state fluorescence polarization results of 1,6-diphenyl-1,3,5-hexatriene in membranes of native and adapted cells are illustrated in Fig. 5. The parameter used, $((r_0/r) - 1)^{-1}$, has previously been demonstrated to be directly proportional to the rotational relaxation time [20], where the term, r_0, represents the maximal limiting anisotropy with an experimental value of 0.362 [21]. In native organisms, the $((r_0/r) - 1)^{-1}$ values are significantly higher for elaidate than for oleate plus palmitate organisms throughout the temperature range studied. This observation indicates that the apparent microviscosity of elaidate membranes is higher than that of oleate plus palmitate. Approximate calculation of viscosity according to the method of Shinitzky and Barenholz [22] results in respective values of 4.6 and 3.5 P at 37°C. For both membrane compositions, plots of log $((r_0/r) - 1)^{-1}$ vs. the reciprocal of the absolute temperature yield biphasic curves with changes in

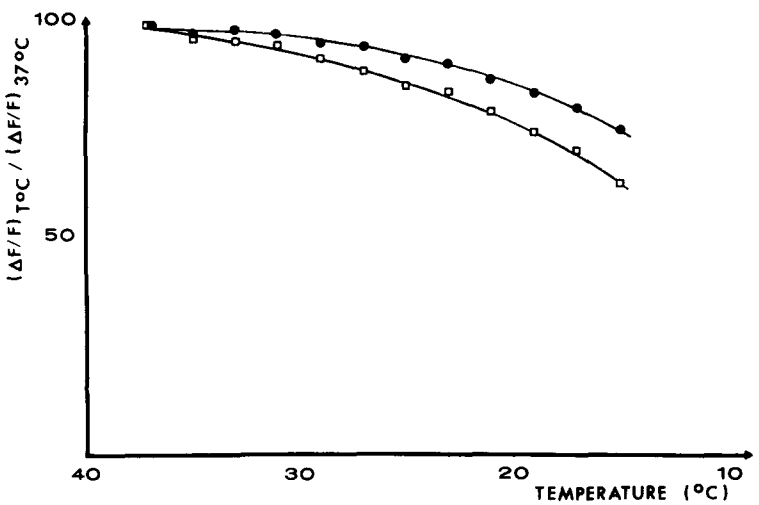

Fig. 3. Effect of temperature on $\Delta\Psi$ in (chol (+)) organisms. Glucose-induced fluorescence intensity quenching at a given temperature $(\Delta F/F)_{t°C}$ divided by the value obtained at 37°C $(F/F)_{37°C}$ (see Methods). □, (chol (+), O + P); ●, (chol (+), E).

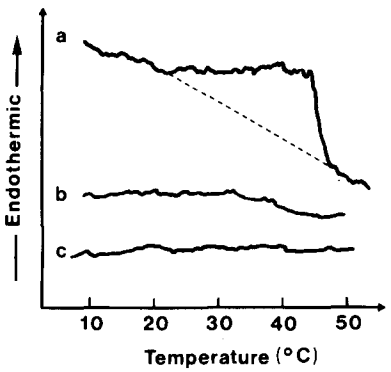

Fig. 4. Thermograms of PG3 membranes. Thick membrane suspensions in diluted β-buffer were scanned at 5° C per min. The lipid phase transition was recorded at a range of 0.5. a, (chol (—), E); b, (chol (+), E); c, (chol (+), O + P).

slopes, and are indicative of the occurrence of a phase separation between 29 and 31°C. Two of the three experiments on elaidate native cell $((r_0/r) - 1)^{-1}$ values at 29°C were comparable to those obtained at 31°C (Fig. 5).

In spite of the presence of non-negligible amounts of membrane lipids in the gel state (as judged from DSC and freeze-fracture experiments), the mean microviscosity of low cholesterol elaidate organisms is significantly lower (η = 3.2 P) at 37°C than that of native cells. This difference rapidly vanishes when the temperature is lowered, so that at 27°C, where a first break occurs, the reverse is observed. A large increase in the $((r_0/r) - 1)^{-1}$ value is further obtained between 21 and 18°C and corresponds to the lower end of the phase transition as detected by DSC.

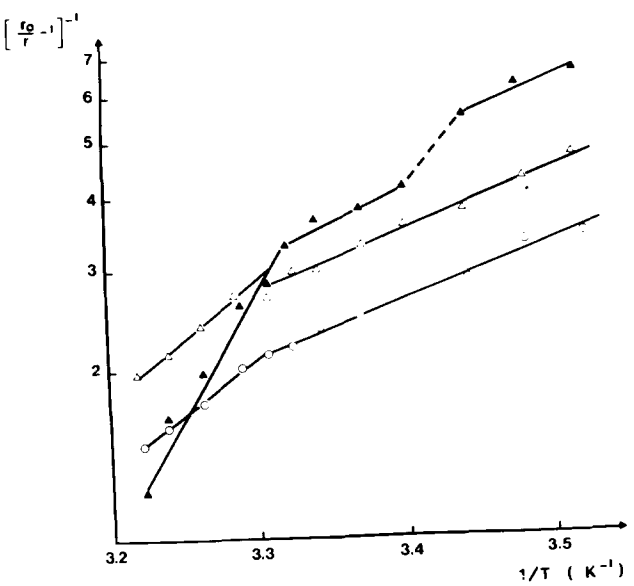

Fig. 5. Temperature dependence of the fluorescence polarization of diphenylhexatriene in PG3 membranes. ○, (chol (+), O + P); △, (chol (+), E); ▲, (chol (—), E). T = absolute temperature $\times 10^{-3}$.

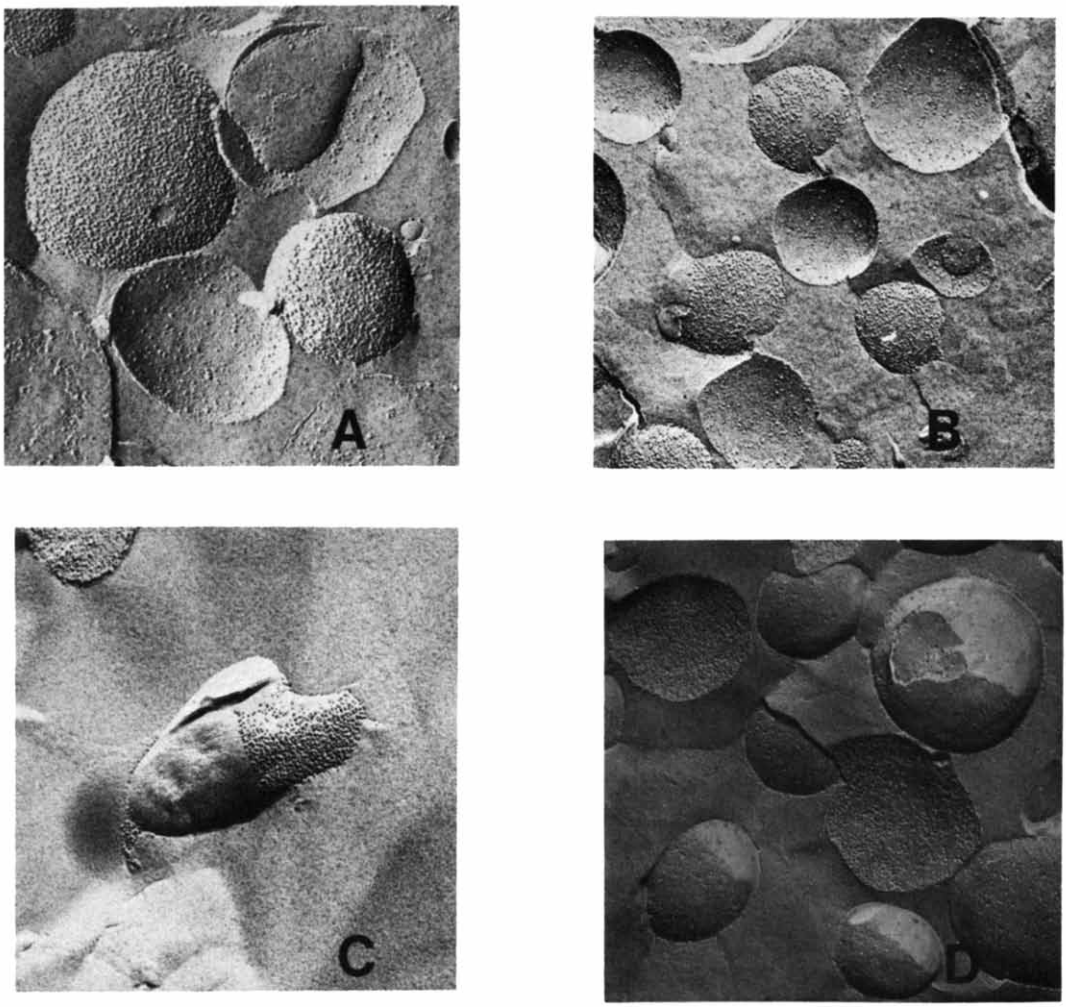

Fig. 6.

Freeze-fracture electron microscopy. At 37°C, the PF face of native organisms grown with oleate plus palmitate always displays uniformly distributed intramembranous particles (Fig. 6a). This distribution is clearly less uniform in the case of native elaidate organisms (Fig. 6b). In accordance with previous results [8], large areas devoid of particles are present in low-cholesterol cells (Fig. 6c) which nevertheless show quite a satisfactory growth rate at this temperature. At 7°C, small areas devoid of particles are observed in native oleic plus palmitic organisms (Fig. 6d). This phenomenon is much more pronounced for normal-cholesterol elaidate cells (Fig. 6e) although no phase separation comparable to that observed in the low-cholesterol adapted organisms can be seen (Fig. 6f).

Finally, no clear difference appears between the particle distribution of native elaidate cells fixed at 37 and 27°C (Fig. 6b, and g).

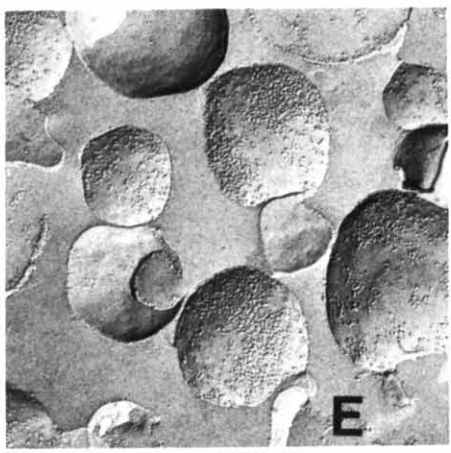

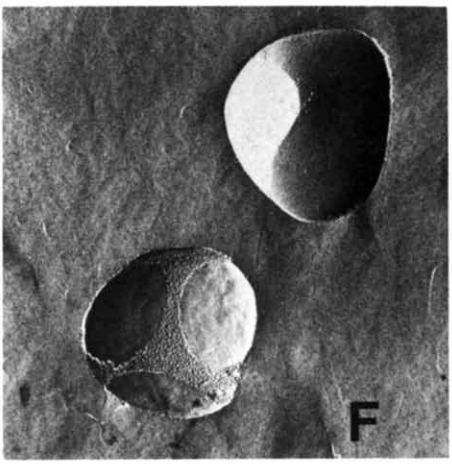

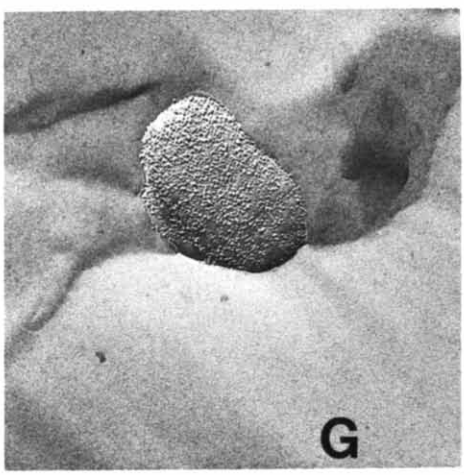

Fig. 6. Freeze-fracture photograph of Mycoplasma PG3. Fixation at 37°C: A, (chol (+), O + P) (×46 800); B, (chol (+), E) (×29 700); C, (chol (—), E) (×37 800). Fixation at 7°C: D, (chol (+), O + P) (×37 800); E, (chol (+), E) (×37 800); F, (chol (—), E) (×37 800); G, (chol (+), E), fixed at 27°C (×37 800).

Discussion

Our measurements of the exchange K^+ active influx as a function of temperature clearly show that in mycoplasma PG3, this influx is affected by changes in the membrane lipid composition. In order to interpret these results, however, it should be kept in mind that K^+ accumulation by this organism is dependent on the existence of a transmembrane potential created through the activity of the membrane-bound Mg^{2+}-ATPase [6]. Factors able to affect ATPase activity, $\Delta\Psi$, or both are therefore also susceptible, a priori, to affect the K^+ transport properties. This is particularly true for the Mg^{2+}-ATPase(s) of mycoplasmas which has repeatedly been shown to be an integral membrane-bound protein the activity of which is dependent on the membrane lipid physical state [18,19,23,25].

Comparison of Arrhenius plots demonstrates that the changes in the K^+

active transport cannot be accounted for by variations in the ATPase activity: for the three membrane compositions studied, a change in the slope of the Arrhenius plots of the Mg^{2+}-ATPase occurs between 28 and 32°C. On the other hand, for K^+ transport we observed: (1) a significant upward deflection for native elaidate-enriched cells; (2) a 'break' at approx. 23°C for adapted organisms; (3) no 'break' for native organisms grown with oleate plus palmitate. The existence of a 'break' in the ATPase activity of adapted organisms at a temperature approx. 10°C higher than that of the lower end of the lipid phase transition as determined by DSC is in accordance with previous data obtained on *A. laidlawii* [25]. Plots of $\log ((r_0/r) - 1)^{-1}$ vs. the reciprocal of the absolute temperature further indicate that this break is associated with a lipid phase separation phenomenon [22]. By analogy with *A. laidlawii* the Mg^{2+}-ATPase activity of which is dependent on phosphatidylglycerol [24], it can be suggested that the observed lipid-phase separation corresponds to the liquid-gel transition of the phospholipid species preferentially associated with the Mg^{2+}-ATPase of the PG3 strain. The presence of 'breaks' in the Arrhenius plots of the ATPase activity of native organisms was not previously detected by Rottem et al. [18]. Comparing our data with theirs, we can postulate that this probably is due to the relatively lower cholesterol content of our membrane preparations. Although the amount of cholesterol in the present experiments is sufficient to reduce the energy content of the transition to an undetectable level by DSC, the fluorescence polarization data indicate that a phase separation or transition must occur at approx. 30°C in our membrane preparations. Freeze-fracture photographs obtained from native cells fixed at 7°C show a non-uniform distribution of intramembranous particles which, although much less pronounced than that observed for low-cholesterol adapted cells, support the hypothesis of a lipid phase change in the range of temperatures studied. A possible exclusion of cholesterol from the environment of the ATPase [26] could have contributed to the observed effect.

It has previously been demonstrated that modifications of the membrane lipid composition can affect the intracellular K^+ level of PG3 organisms via an effect on $\Delta\Psi$ [8]. However, comparison of the K^+ transport and glucose-induced merocyanine fluorescence quenching curves clearly shows that the K^+ active influx temperature-dependent patterns are not due to parallel variations in $\Delta\Psi$. In accordance with the ATPase data, the decrease in $\Delta\Psi$, although limited, becomes more pronounced for temperatures below 30°C. The effects of temperature variations on the glucose-induced fluorescence quenching are, however, less marked than those of the ATPase activity. We can hypothesize that lowering the temperature would result in a decreased H^+ permeability and consequently, in the proton backflux. This in turn would increase the efficiency of the proton pump and result in a partial compensation for the decrease in the ATPase activity. The finding that $\Delta\Psi$ is less sensitive to temperature variations in the elaidate organisms, the membrane microviscosity of which is enhanced, supports this hypothesis.

The lack of a direct correlation between the variations in either the Mg^{2+}-ATPase activity or $\Delta\Psi$ and the K^+ active influx seems to indicate that in PG3 the K^+ carrier cannot be identified with the Mg^{2+}-ATPase. This contrasts with recent data obtained on *E. coli* showing that a K^+-stimulated membrane ATPase

serves as the K^+ carrier in the K^+-dependent system [27,28]. Although the possibility of the existence of another membrane-bound ATPase species cannot be excluded, a priori, it seems unlikely in view of our previous experiments which failed to demonstrate any K^+-stimulated ATPase activity [6].

Independently of its nature, our results strongly suggest that the changes in the membrane lipid composition affect the K^+ transport at the level of the carrier itself. This effect cannot be explained in terms of a specificity towards a fatty acid species or a concentration of cholesterol in the membrane: native or adapted elaidate-enriched organisms have a comparable membrane fatty acid composition but show a quite different pattern for the temperature dependence of K^+ active influx. This holds true for native organisms of which the cholesterol concentration is comparable but of which the fatty acid composition differs. This is more than likely due to the associated changes in the membrane microviscosity. This is supported by the fluorescence polarization data which show that the microviscosity of native cells is higher for elaidate than for oleate plus palmitate enriched organisms. For example, it can be calculated from Fig. 5 that the microviscosity of elaidate membranes at 31°C is equivalent to that of oleate plus palmitate at 15°C. The observation in low-cholesterol elaidate cells of a 'break' in the K^+ active influx at a temperature corresponding to the lower end of the lipid phase transition further suggests that in contrast with the ATPase(s), the K^+ carrier is associated with the more fluid lipid species. Although this would explain the absence of a 'break' in the Arrhenius plot of K^+ active influx of oleate plus palmitate enriched organisms, additional hypotheses are needed to explain the results obtained on native elaidate cells. One must first admit that the presence of cholesterol, even at a suboptimal concentration, increases the microviscosity of those fluid lipid species surrounding the K^+ carrier. Such an assumption appears reasonable in view of results obtained on model systems showing that cholesterol preferentially interacts with the most fluid species in mixtures of synthetic phospholipids [29]. Secondly, because the existence of a discontinuity in Arrhenius plots is only evident for K^+ active transport it must originate from a local event that affects the K^+ carrier itself. As the temperature at which it occurs corresponds to that of the phase separation it could originate from the existence of boundary zones between a lipid species in the gel phase and the most fluid lipid species of the membrane. A defect in membrane organization brought on by such a situation could favor the activity of the K^+ carrier [30]. Finally, the absence of a deflection for native organisms grown on oleic plus palmitic acids would result from the higher degree of fluidity of the membrane, thus allowing a sufficient penetration or motion of the K^+ carrier.

In conclusion, the present experiments support the idea that in PG3 organisms, the K^+ carrier is associated with the lower melting lipid species and is sensitive to modifications in their microviscosity state. Combined with our previous work [8], this implies that both active K^+ influxes and intracellular steady-state K^+ levels are dependent on the membrane lipid composition. The mechanisms involved are however completely different as the effect on intracellular K^+ levels is indirect and primarily mediated by modifications of $\Delta\Psi$.

Acknowledgements

This work was supported in part by the Kidney Foundation of Canada. C.L.G. is a scholar of the Conseil de la Recherche en Santé du Québec. We wish to thank Mrs. Michèle Lucarain and Mrs. Marie Cécile Giocondi for their excellent technical assistance and Mrs. Louise Lefort and Mrs. Rose Warnock for their secretarial skills.

References

1 Singer, S.J. (1974) Annu. Rev. Biochem. 43, 805—833
2 Melchior, D.L. and Stein, J.M. (1976) Annu. Rev. Biophys. Bioenerg. 5, 205—238
3 Overath, P., Thilo, L. and Traüble, H. (1976) Trends Biochem. 1, 186—189
4 Sandermann, H. (1978) Biochim. Biophys. Acta 515, 209—237
5 Leblanc, G. and Le Grimellec, C. (1979) Biochim. Biophys. Acta 554, 156—167
6 Leblanc, G. and Le Grimellec, C. (1979) Biochim. Biophys. Acta 554, 168—179
7 Rottem, S., Yashouv, J., Ne'Eman, Z. and Razin, S. (1973) Biochim. Biophys. Acta 323, 495—508
8 Le Grimellec, C. and Leblanc, G. (1978) Biochim. Biophys. Acta 514, 152—163
9 Razin, S. (1963) J. Gen. Microbiol. 33, 471—475
10 Rottem, S., Stein, O. and Razin, S. (1968) Arch. Biochem. Biophys. 125, 46—56
11 Biais, R. (1975) Anal. Chem. 63, 271—273
12 Chen, R. and Bowman, R. (1965) Science 147, 729
13 Shinitzky, M., Dianoux, A.C., Gitter, C. and Weber, G. (1971) Biochemistry 10, 2106—2113
14 Bligh, E.G. and Dyer, W.J. (1959) Can. J. Biochem. Physiol. 37, 911—917
15 Metcalfe, L.D., Schmitz, A.A. and Pelka, J.R. (1966) Anal. Chem. 38, 514—515
16 Wycoff, H.D. and Parsons, J. (1957) Science 125, 347—348
17 Lowry, O.H., Rosebrough, N.J., Farr, A.L. and Randall, R.J. (1951) J. Biol. Chem. 193, 265—275
18 Rottem, S., Cirillo, V.R., de Kruijff, B., Shinitzky, M. and Razin, S. (1973) Biochim. Biophys. Acta 323, 509—519
19 De Kruijff, B., van Dijck, P.W.M., Goldbach, R.W., Demel, R.A. and van Deenen, L.L.M. (1973) Biochim. Biophys. Acta 330, 269—282
20 Shinitzky, M. and Inbar, M. (1976) Biochim. Biophys. Acta 433, 133—149
21 Shinitzky, M. and Barenholz, Y. (1974) J. Biol. Chem. 249, 2652—2657
22 Shinitzky, M. and Barenholz, Y. (1978) Biochim. Biophys. Acta 515, 367—394
23 Hsung, J.C., Huang, L., Hoy, D.J. and Haug, A. (1974) Can. J. Biochem. 52, 974—980
24 Bevers, E.M., Snock, G.T., op den Kamp, J.A.F. and van Deenen, L.L.M. (1977) Biochim. Biophys. Acta 467, 346—356
25 Jinks, D.C., Silvius, J.R. and McElhaney, R.H. (1978) J. Bacteriol. 136, 1027—1036
26 Warren, G.Z., Housley, M.D., Metcalfe, J.C. and Birdsall, N.J.M. (1975) Nature 255, 684—687
27 Epstein, W., Whitelaw, V. and Hesse, J. (1978) J. Biol. Chem. 253, 6666—6668
28 Wieczorek, L. and Altendorf, K. (1979) FEBS Lett. 98, 233—236
29 Van Dijck, P.W.M., de Kruijff, B., van Deenen, L.L.M., de Gier, J. and Demel, R.A. (1976) Biochim. Biophys. Acta 455, 576—587
30 Linden, C.D., Wright, K.L., McConnel, H.M. and Fox, C.F. (1973) Proc. Natl. Acad. Sci. U.S.A. 70, 2271—2275